10.1071/EN23033
Environmental Chemistry

Supplementary Material

Robust calculus for biotransformation in wastewater generalised across thousands of chemicals and conditions

Tom M. Nolte[A,*], *Willie J. G. M. Peijnenburg*[B,C] and *Peter L. A. van Vlaardingen*[B]

[A]Department of Environmental Science, Institute for Water and Wetland Research, Radboud University Nijmegen, 6500 GL Nijmegen, Netherlands

[B]National Institute for Public Health and the Environment (RIVM), Centre for Substances and Integrated Risk Assessment (SIR), 3720 BA Bilthoven, Netherlands

[C]Institute of Environmental Sciences (CML), Leiden University, PO Box 9518, 2300 RA, Leiden, Netherlands

*Correspondence to: Email: tom.m.nolte@gmail.com

Parameter	Meaning	Value	Unit
	Speciation		
$pH_{influent}$	Acidity of the influent		unitless
pB	Buffering capacity		unitless
pH	Acidity of the medium in the aeration tank		unitless
pK_a	Acid dissociation constant of CEC		unitless
$\Delta G_{BOD}^{\ddagger}$	Activation energy for degradation of BOD	25	$kJ \cdot mol^{-1}$
c_{BOD}	Stoichiometric conversion factor for conversion of BOD to H^+	1	unitless
$[BOD]$	Biological oxygen demand of influent		$kg \cdot L^{-1}$
T	Temperature		Kelvin
R	Ideal gas constant	$8.314 \cdot 10^{-3}$	$kJ \cdot mol^{-1} \cdot Kelvin^{-1}$
	Sorption		
$[COD]$	Chemical oxygen demand in primary influent		$kg \cdot L^{-1}$
$[TSS]$	Concentration of total bio-inactive suspended solids in primary influent		$kg \cdot L^{-1}$
$K_{TSS/W}$	Equilibrium constant for sorption of CEC to TSS		$L \cdot kg^{-1}$
$K_{OM/W}$	Equilibrium constant for sorption of CEC to organic matter in TSS		$L \cdot kg^{-1}$
$\Delta G_{OM/W}$	Free energy for sorption of CEC to organic matter in TSS		$kJ \cdot mol^{-1}$
ΔG_h	Hydrophobic component of $\Delta G_{OM/W}$		$kJ \cdot mol^{-1}$
$\Delta G_{\pm}$	Ionic exchange component of $\Delta G_{OM/W}$ for cationic CECs	5.5	$kJ \cdot mol^{-1}$
f_{OM}	Fraction of TSS that contains carbon	1	unitless
ρ	Density of TSS	1.4	kgL^{-1}
h_{OM}/h_{Oct}	Effectivity of hydrophobic binding to TSS over octanol	0.3	unitless
$\Delta G_{Oct/W}$	Free energy of moving a CEC from water phase to octanol phase		$kJ \cdot mol^{-1}$
$K_{TSS/W,CECn}$	Equilibrium constant for sorption of neutral CEC species to TSS		$L \cdot kg^{-1}$
$K_{TSS/W,CECion}$	Equilibrium constant for sorption of charged CEC species to TSS		$L \cdot kg^{-1}$
$K_{OM/W,CECn}$	Equilibrium constant for sorption of neutral CEC species to OM		$L \cdot kg^{-1}$
$K_{OM/W,CECion}$	Equilibrium constant for sorption of charged CEC species to OM		$L \cdot kg^{-1}$
	Biodegradation		
$\Delta G_{EFSA}^{\ddagger}$	Average EFSA activation energy	65.4	$kJ \cdot mol^{-1}$
$\Delta G_{CEC,redox}^{\ddagger}$	Redox-dependent contribution of CEC to average EFSA act. energy		$kJ \cdot mol^{-1}$
k_{CEC}	2^{nd} order rate constant for biodegradation of CEC		$L \cdot mol^{-1} hr^{-1}$
k_{EFSA}	Log-average 2^{nd} order rate constant for biodeg. of CECs by EFSA		$L \cdot mol^{-1} hr^{-1}$
A_{CEC}	Frequency factor of CEC		$L \cdot mol^{-1} hr^{-1}$
A_{EFSA}	Log-average frequency factor of CECs by EFSA		$L \cdot mol^{-1} hr^{-1}$
HRT	Hydraulic retention time of the mixing aeration tank		hours
$k_{CEC,n}$	2^{nd} rate constant for biodegradation of neutral CEC species by QSPR calc.		$L \cdot mol^{-1} hr^{-1}$
$k_{CEC,ion}$	2^{nd} rate constant for biodegradation of charged CEC species by QSPR calc.		$L \cdot mol^{-1} hr^{-1}$
$k_{CEC,QSPR}$	Apparent 2^{nd} rate constant for biodeg. of CEC as function of pH (QSPR calc.)		$L \cdot mol^{-1} hr^{-1}$
$k_{EFSA,QSPR}$	Average 2^{nd} order rate constant for EFSA CECs by QSPR calculation		$L \cdot mol^{-1} hr^{-1}$
	Acclimation		
v_{CEC}	Stoichiometric ratio for production of active CEC-degrading biomass		unitless
$[CEC]_{influent}$	Concentration of CEC in the WWTP influent		$mol \cdot L^{-1}$
$[CEC]_{EFSA}$	Log-average of concentration of CECs as used by EFSA in biodeg. exps.	$3 \cdot 10^{-6}$	$mol \cdot L^{-1}$
$[CEC]_W$	Concentration of CEC in the mixing aeration tank		$molL^{-1}$
$[E_{CEC}]$	Active CEC-degrading biomass induced by CEC		$mol \cdot L^{-1}$
$[CEC]_{effluent}$	Concentration of CEC in the effluent water of the aeration tank		$mol \cdot L^{-1}$
k	1^{st} rate constant for biodegradation of CEC in aeration tank		$hours^{-1}$
Removal	Percentage of [CEC] removed by biodegradation in the aeration tank		%
β	Microbiota diversity	Fitted result	unitless
k_{50}	1^{st} order rate constant at which aerobic tank removes 50% of [CEC]	Fitted result	$hours^{-1}$

Contents

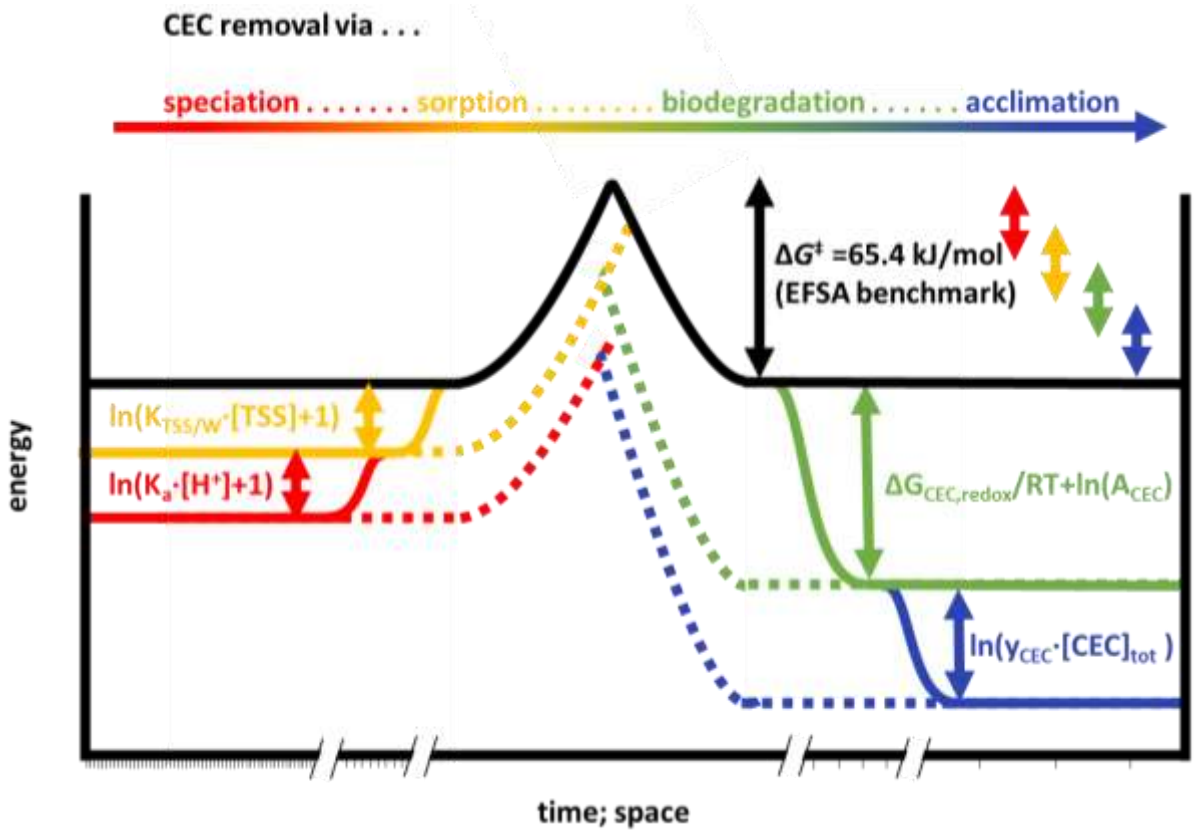

Figure S1. Schematic representation of the processes parametrized in this study. Tick marks on the x-axis represent 4 different temporal domains (not to scale) over which the local equilibrium assumption (LEA) assumption was applied.

S1. Acidity (fastest)

According to the local equilibrium assumption (LEA), we describe the parametrization of the fastest process first [1]. We assume that, with respect to sorption (*Section S2*), pH speciation is effectively instantaneous. In absence of (in situ) experimental (monitoring) data for pH and buffering (B) capacity, we calculated the pH according to:

Eq. S1 $$pH = pH_{influent} + (\Delta_{HRT} pH - pB)$$

The endemic pH ($pH_{influent}$) of the wastewater is 7.4-7.8 under which, on average, all WTTPs (optimally) operate.

The pH values, however, are subject to changes as a result of nitrification prior or during the treatment [2, 3]). E.g., nitrification (oxidation) of NH_4^+ produces H^+,

Eq. S2 $$2NH_4^+ + 4O_2 \rightarrow 2NO_3^- + 2H_2O + 4H^+$$

and decomposition of organic carbon produces carbon dioxide as an oxidation product: $CO_x+O_2 \rightarrow CO_2+xO$, with a maximum stoichiometry (c) of 1, and rates related to the oxidation state (~x) of BOD (2±2) in wastewater, relative to CO_2 (4). The influence of temperature on Eq. S2 is equivalent to that of $\Delta G^{\ddagger}_{met}/RT$ (Eq. S6). CO_2 in turn can acidify the wastewater via Eq. S3-5, intricately linking pH, BOD and N status:

Eq. S3 $$CO_2(\uparrow) + H_2O \rightleftharpoons H_2CO_3$$

Eq. S4 $$CO_2(\uparrow) + H_2O + CO_3^{2-} \rightleftharpoons 2HCO_3^-$$

Eq. S5 $$CO_2(\uparrow) + OH^- \rightleftharpoons HCO_3^-$$

in which all species participate with stoichiometries c of 1.

pH and dissolved O_2 determine the redox state of the wastewater; hence, $[O_2]$ and O_2 consumption are indicators of pH. Therefore, we calculated acidity (pH) changes (Δ) from changes in BOD, including changes in concentrations of NH_4^+ [4, 5]. We assume O_2 levels to be in excess and constant, so that BOD corresponds to C/N to be oxidized.

We determined the effective stoichiometries c for $[H^+]$ production in wastewater treatment semi-empirically, by solving rate equations:

Eq. S6 $$10^{\Delta_{HRT} pH - pB} = \int [H^+](t)\, dt \propto e^{-(\frac{\Delta G^{\ddagger}_{BOD}}{RT})} \cdot [BOD]^{c_{BOD}}$$

Wherein $[O_2]$ is in excess (hence, irrelevant). We take a factor ~2 bacterial metabolic activity (respiration, metabolism) increase per 15°C, i.e., an apparent average 'activation energy' $\Delta G^{\ddagger}_{BOD}$ = 25±5 kJ/mol [6-8] (lower, i.e., more efficient, than a 'universal' 50-60 $kJmol^{-1}$ [9, 10] (*Section S3*) implying specialized oxidation of (mostly) organic carbon in WWTPs under 'normal', i.e., equilibrated (optimized/acclimated) conditions. The narrow margin of $\Delta G^{\ddagger}_{BOD}$ represents a constant BOD type to which bacteria have uniformly adapted (i.e., no in situ phase changes [11]). BOD consisting of lipids, carbohydrates, etc. [12]. c_{BOD} is the stoichiometric coefficient, obtained by comparing:

Eq. S7 $$\Delta_{HRT} pH - B = c_{BOD} \cdot \log(\Delta_{HRT}[BOD])$$

We take as shape of $\int [H^+](t)$ and $\int [BOD](t)$, the temporal evolution of pH&BOD in the reactors (Eq. 6), exponential decay (analogous to CEC degradation in WWTP pseudo-steady state, S2.4).

Acidification in situ also depends on the buffering capacity B of wastewater. We neglect temperature influences on (bicarbonate) buffering. To accurately parametrize the influences of Reactions 3-5, B needs to be taken into account. Wastewater characterization lacked info on B (e.g., alkalinity), we assume the contribution from BOD and TSS to B is constant among reactors. We assume that CEC concentrations (µg/L) do not influence B.

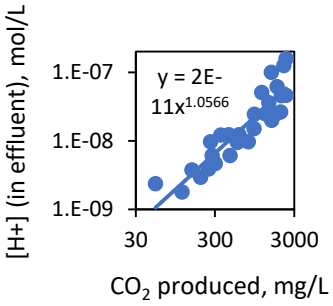

Fig. S2 Parametrizing pH and buffering effects in WWTPs. We constructed the relationships analogous to Lijklema et al. [2, 13] (BOD = 0.3COD) and implemented c=1. CO_2 production correlates with ammonia oxidation.

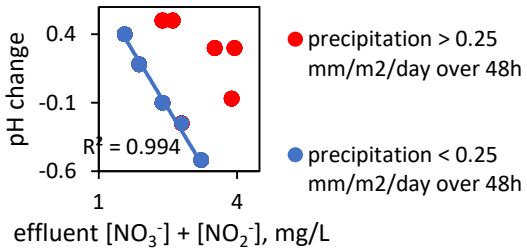

Fig. S3. pH change following wastewater treatment (performance in terms of effluent nitrate and nitrite). Data from [14].

EPA states a maximum of 44 kgCO_2 per 32 kgBOD [15], c=1.00. Hence, studies applied 1.375 kg CO_2/kg BOD [16] (i.e., a 1:1 mol ratio: c=1.00) [17]. Larger BOD/COD particles are more difficult to degrade by microorganisms i.e., they have a lower CO_2 yield (require more O_2). Oxidation of organic matter may produce 0.986 gCO_2/gBOD [18], in mol this implies c = (0.986/44))/(1/32) = 0.72. Others found 0.95 kgCO_2/kgBOD for carbon respiration (c=0.69) [19]. Eq. S7 gave c=1.05±0.10, Fig. S2. We thereby applied values of c = 1 for a homogeneous system. With c we calculated free $\Delta[H^+]$ changes, i.e., 10^{pH}.

c values (at/close to theoretical maximum of 1.00) imply that within operation conditions the volatilization amounts (stripping, Fig. S4) of CO_2 are negligible as compared to the amounts produced [20, 21]; Fig. S2 [22]. This underpins the aquaphilic character of CO_2, e.g. Henry constant [23], and water/air partitioning (*K*) of ~30 (0.015·*K*+1 = (33%+4.5%)/33%, (0.015 = ocean/atmosphere volume ratio: $3x10^8$miles/$2x10^{10}$miles) (2.3mmol CO_2 /kg seawater, hence, 2.3 mmol CO_2/55.55 mol), thus minor release of CO_2. In stabilization ponds (Fig S4) pH change is reversed due to CO_2 evaporation: higher ΔBOD, more CO_2 to be evaporated, more pH increase. Volatilizations of both CO_2 and CECs can be considered in future assessment.

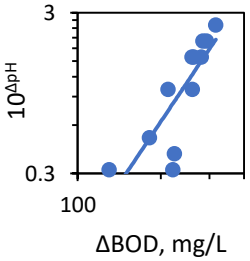

Fig. S4. pH change following BOD changes in wastewater stabilization ponds (HRT = 3.5-20.5 days). Data from Mansouri [24].

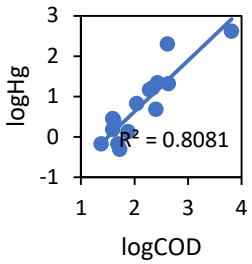

Fig. S5. Refinery wastewater concentrations of mercury (y) and COD (x).

S2. Bioavailability/Sorption (fast)

SimpleTreat uses a single (time-independent) value for TSS (to which CECs) sorb. We implement TSS to calculate free (i.e., bioavailable) concentrations according to [25, 26]:

Eq. S8 $$[CEC]_W = \frac{[CEC]_{influent}}{K_{TSS/W} \cdot [TSS] + 1}$$

BOD needs no bioavailability calculation as it is homogeneous. We take that 90% of TSS are removed during primary treatment [27-29]. We take TSS (kg/L) concentrations from [14] via $[TSS] = 1.5 \cdot \frac{[COD] - 45.0}{2.8} - 5.4$ [30]. We assumed binding exclusively to organic TSS (OM) in standard activated sludges and raw sewage for all WWTPs (i.e., negligible sorption to e.g., minerals). We assume that, with respect to biodegradation (*Section S3*), sorption is effectively instantaneous. Hence, accountable via equilibrium partitioning and Henderson-Hasselbalch. We calculated K_{TSS} (L/kg) via $K_{TSS} = f_{OM} \ K_{OM/W}/\rho$ (i.e., $\log K_{TSS} = K_{OM/W} + \log f_{OM} - \log \rho$), with density ρ=1.4 kg/L [31]. Since approximately all TSS contains carbon, we take f_{OM} = 1. As aerobic tanks are well-mixed, we also assume that sorption will be in effective equilibrium before any significant biodegradation can take place in WWTPs. We obtained $K_{OM/W}$ (kg OC / L water) from:

Eq. S9 $$K_{OM/W}(pH) = \frac{K_{OM/W,CEC_n}}{1+10^{a(pK_a - pH)}} + \frac{K_{OM/W,CEC_{ion}{}^{ion}}}{1+10^{a(pH - pK_a)}}$$

Wherein K's are partitioning, pH is the acidity, a is 1/-1 for (basic/acidic CECs), see *Section S1*.

We assume that any change in enthalpy after sorption as a function of compound characteristics is offset by entropy changes ($\Delta H_{OM/W} = T\Delta S_{OM/W} + \Delta G_{OM/W}$). See e.g., the strong correlations between enthalpy and entropy [32, 33]. We thus need not distinguish between entropy/enthalpy differences, and hence describe temperature effects via a Boltzmann distribution:

Eq. S10 $$\log K_{OM/W} = -\frac{\Delta G_{OM/W}}{2.303RT}$$

With R = $8.314 \cdot 10^{-3}$ $kJmol^{-1}K^{-1}$, and wherein we calculated Δ*G* (kJ/mol) from:

Eq. S11 $$\Delta G_{OM/W} = \Delta G_{\mathrm{h}} + \Delta G_{\pm}$$

We approximated hydrophobic ΔG_h binding energy values, via $\Delta G_{\mathrm{h}} = \frac{h_{OM}}{h_{Oct}} \Delta G_{Oct/W}$, via octanol/water (Oct/W) partitioning $K_{Oct/W}$ values [34] which we assumed were scaled to standard conditions, i.e., correspond to a standard concentration [35] and T≈15°C (hence, $\Delta G_{OM/W} = -0.0592 \cdot \log K_{OM/W}$). ($h_{OM}/h_{Oct}$) represents the effectivity of hydrophobic (inverse polar) binding to organic material (i.e., TSS) over octanol. $\Delta G_{\pm}$ represents ionic binding.

Sorbent-sorbate geometry affects ΔG_h and $\Delta G_{\pm}$. However, WWTP managers/operators do not (continuously) monitor structures of relevant colloids in sludge. We take a single homogenous type of OM, and a single binding mode. Empirically, we obtained h_{OM}/h_{Oct} = 0.3 (Fig. S6). Carbon contents of 0.37 and 0.3 [36-38] apply for activated sludge and raw sewage, Fig. S6. Octanol has ~3.5x more fractional hydrophobic surface area (TSA/TPSA ≈ 2 and 7) available for binding then organic materials/molecules, e.g., humic acid (brown) and octanol (yellow, Fig. S6), substantiating h_{OM}/h_{Oct} = 0.3 [39], similar to 0.23 [40]. We thereby applied (h_{OM}/h_{Oct}) = 0.3. For organic cations we take $\Delta G_{\pm}$ = 5.5 kJ/mol ($\log K \cdot (2{,}303 \cdot R \cdot T) = 1 \cdot 2.303 \cdot 8.314 \cdot 288/1000 = 5.5$ kJ/mol, Fig. S6), representing physical adsorption due to (weak) ion exchange (e.g., metals complexed by organic molecules 6 kJ/mol [41-44] to e.g., phenolic and carboxylate groups.

Regression slope and offset for anionic (red, Fig S6) compounds are identical to those for neutral (black, Fig S6) compounds (within standard error). For cations, the slope of the regression between $logK_{oct/w}$ and $logK_{om/w}$ is similar to the slope for neutral and anionic compounds (Fig. S6): because the compounds have a similar hydrophobic binding mode. At low $K_{oct/W}$, the regression slope may be low since CECs do not bind to hydrophobic OM [45]. Empirically, however, the binding seems to occur to a mostly uniform binding matrix, meaning there is low heterogeneity in hydrophobicity within OM [46]), Fig. S6. Thereby, we assumed a single OM type. Regression slopes in [47] are dissimilar (0.47 for cations, 0.11 for anions), which is explained by the fact that Franco and Trapp used $K_{oct/w}$ for the neutral molecule, whereas we used the $K_{oct/w}$ for molecule as they are (de)protonated at pH7.4.

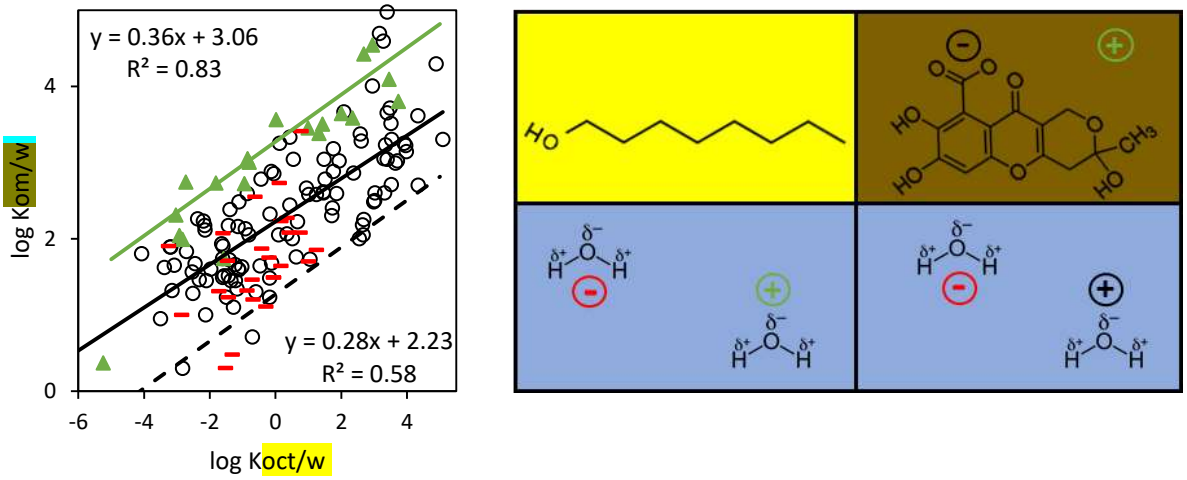

Figure S6. Organic material/water ($K_{OM/W}$) partitioning (y) estimated from octanol/water partitioning (x). Red=anions, Green=cations, Black=neutrals (>50%). Experimental $K_{OM/W}$ values taken from [47] which we assume describe a constant density for OM, so that $K_{OM/W}$ values (L/kg) are directly proportional to values for partitioning (unitless), hence do not affect parametrization.

S3 Biodegradation (slow)

We take pH speciation and sorption equilibration as instantaneous relative to biodegradation. We describe biodegradation of CECs therein according to:

Eq. S12 $$removal \equiv \frac{[CEC]_w}{1+k \cdot HRT}$$

With k as a first order biodegradation rate constant (hr^{-1}), equivalent to those obtained from standardized biodegradability tests, e.g., OECD 301, 309 [48, 49] (wherein $k \cdot HRT=(k/k_{50})^{\beta}$). We calculated biodegradation by assuming that chemical transformations occur via second order kinetics:

Eq. S13 $$k = k_{CEC} \cdot [E_{CEC}]$$

Wherein $[E_{CEC}]$ (e.g., in mol/L or cells/L) is the effective biomass is (equivalent to $v_{CEC} \cdot [CEC]_{influent}/(K_{TSS/W} \cdot TSS+1)$, see *Section S2;S4*), with $k_{CEC} = A_{CEC} e^{-(\frac{\Delta G^{\ddagger}_{CEC}}{RT})}$[50]. We take activation energies $\Delta G^{\ddagger}_{CEC}$ as 'apparent' values, by way of an active average for the range of enzymes etc. present, and obtained it from:

Eq. S15 $$\Delta G^{\ddagger}_{CEC} = \Delta G^{\ddagger}_{EFSA} \pm \Delta G^{\ddagger}_{CEC,redox}$$

In which we took for the reference value $\Delta G^{\ddagger}_{EFSA}$ = 65.4 kJ mol^{-1}. This value is a median $\Delta G^{\ddagger}$ for neutrally-charged contaminants [50] with a 90% probability within 45.8-93.3 $kJmol^{-1}$. The value corresponds to a compound among the <5% most difficult to metabolize under conventional O_2 respiration [51].

According to Boltzmann, a 20 kJ/mol variation corresponds to a ~10^4 population ratio; this value represents uptake enhancement (of BOD nutrients over CECs pollutants) [52, 53]. Lipids and carbohydrates have K_{OM} values of $10^{5\pm5}$, on average ~10^4 times higher than CECs $10^{0.9\pm4.6}$ [34, 53](S2). The 90% probability relates partially to variance in chemical structure: an apparent mean of $\Delta G^{\ddagger}$ for 84 heterogeneous (anionic, cationic, neutral, etc.) compounds (CEC) is 71(±4) kJ mol^{-1}. The variance (±2SD) corresponds to a factor ~6 (= $e^{-4/RT}$) effect on k_{CEC} at 15°C. We thereby calculated the 'perturbation' $\Delta G^{\ddagger}_{CEC,redox}$ due to variation in chemical structure:

Eq. S16-A $$\Delta G^{\ddagger}_{CEC,redox} = -RT \cdot ln\left(\frac{k_{CEC,QSPR} \cdot k_{EFSA,QSPR}}{A_{CEC} \cdot A_{EFSA}}\right)$$

wherein we calculated preexponential 'frequency' factors A_{CEC} (e.g., $Lmol^{-1}h^{-1}$) by the method in [54] (wherein units h^{-1}; dividing by concentration (e.g., mol/L). The corresponding $k_{EFSA,QSPR}$ and A_{EFSA} are averaged values of CECs evaluated by EFSA [50] obtained by chemoinformatic calculation [54]. We thereby implement the dependence of k_{CEC} on temperature via the Arrhenius equation wherein we take k_{CEC} as an apparent value. We calculate the apparent $k_{CEC,QSPR}$ from rate constants for different protonation (speciation) states:

Eq. S16-B $$k_{CEC,QSPR} = \frac{k_{CEC_n}}{1+10^{a(pK_a-pH)}} + \frac{k_{CEC_{ion}}}{1+10^{a(pH-pK_a)}}$$

We obtained rate constant values $k_{CEC,n}$ and $k_{CEC,ion}$ ($Lmol^{-1}h^{-1}$) at T≈15°C and for biodegradation by chemoinformatic calculation from a quantitative structure-property relationship (QSPR) model from Nolte et al. [54, 55]. Though bacteria can buffer to their own (internal) optimal (working) pH (range), pH can shift in the medium [56]). We assumed that the k values as obtained from the QSBR model represent a (reference) temperature (T_1) of 15°C (i.e., are k_1), and negligible back-transformation

(reverse) (i.e., k' for CEC' → CEC not significant compared to CEC' → CEC'') . We assume that A_{CEC} values are independent of temperature:

Eq. S17

$$k_{CEC,T_2} = k_{CEC,T_1} e^{-\left(\frac{\Delta G^{\ddagger}_{CEC}}{R}\left(\frac{1}{T_2}-\frac{1}{T_1}\right)\right)}$$

S4 Biomass acclimation (slowest)

When running a steady-state model such as SimpleTreat, *k* values entered need to account for acclimated biomass, which is often unknown. We do not differentiate between adaption processes: either via increase of degrader biomass (e.g., Monod growth with lag phases of days), or evolvement of enzymes (over 'long' time scales Δt, e.g., over months) capable of attacking CECs. The apparent $\Delta G^{\ddagger}$ decrease with increasing equilibrated acclimation [11]. Concentrations of CECs in WWTPs can vary by orders of magnitude temporally (e.g., higher use and concentration of the antipsychotic/depressant clopazine in winter than in summer [14, 57]). This can differentially induce acclimation: 'biomass cofactors' [E_{CEC}] which (further) stimulate CEC breakdown.

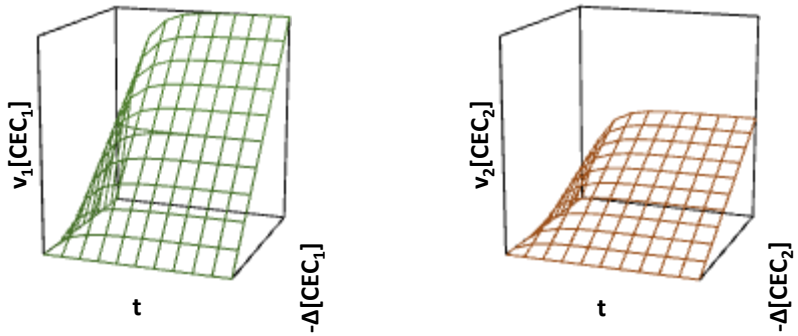

Fig. S7. Consumption of CEC, i.e., -Δ[CEC] (z-axis), can over time (x-axis) induce 'biomass cofactors' [E] (y-axis). [E]/Δ[CEC] is not a function of t anymore at large Δt (e.g., months), mathematically Δt -> ∞. We parametrize the relationship between Δ[E]/Δ[CEC] at large t to describe acclimation. In this illustrative example, $v_{CEC1} > v_{CEC2}$ (green vs. red).

We take that biodegradation is effectively instantaneous as compared to acclimation. We take that acclimation taking place within the 'small' HRT (i.e., within dt) is not significant as compared to acclimation (established) that has occurred (occurring) over months (over Δt), Fig. S7. Varying CEC concentrations between subsequent (variable) HRTs does not significantly effectuate enhancement in E because microbial acclimation is a slower process (e.g., multiple SRTs). In other words, we assume that biomass E metabolizing CECs is in effective steady-state.

Elements (in a wider sense, 'information') of the CEC 'partition' into biomass via a yield v leaving an imprint in terms of genetic material. Depending on stoichiometry, this partitioning increases entropy and lowers free energy [58]. The stoichiometric comparison with BOD captures cometabolism [57]. In ΔG = ΔH – TΔS, higher T enables acclimation, in turn responsible for, when bacteria are in a new 'equilibrium', more negative Δ*G* and lower $\Delta G^{\ddagger}$. We assume that T has no effect on acclimation (Δ[E]/Δ[CEC]) within large Δt (acclimation times), Fig.S7. Experimental values for acclimation in WWTP(-like) conditions are scarce. Instead, we assess acclimation via yields (v) by solving stoichiometric equations ($v_{CEC} \in c[CEC] + x[X] \rightarrow e[E_{CEC}]$). We take E_{CEC} to be induced via the machinery involved in carbohydrate, nucleic and amino acid metabolism (details in [57]). We thereby calculated [E_{CEC}] according to [57]:

Eq. S18
$$\Delta[E_{CEC}] = \Delta(v_{CEC} \cdot [CEC]_W)$$

With $\Delta[CEC]_W$ the CEC concentration that was lost during biodegradation in the secondary aerobic tank. We performed regression (Figs 5;6) to give k_{50} and β values which are indicative of biomass and represent 5×10^{10} cells/L as a representative average for background concentration of biomass $[E]_b$ in WWTP wastewater [59] degrading CECs [55]. v_{CEC} is a unitless stoichiometric ratio representing effective yield for biomass cofactors E_{CEC} involved in degrading CECs [57].

For our modelling, we assume that real-time concentrations [CEC] measured in WWTP influent are (proportional to/representative of) long-term background concentrations as well: given that $\frac{d(\Delta[CEC])}{dt} = \frac{\Delta[CEC]}{\Delta t} + \frac{d[CEC]}{dt}$ (with d/dt in the order of hours or days: HRT), we assume $\frac{\Delta[CEC]}{\Delta t}(t \to inf) = \frac{d[CEC]}{dt}(t \to \inf)$, so that concentrations measured translate into E_{CEC}. Implicitly, as a result: $\frac{d[E_{CEC}]}{dt} = \frac{\Delta[E_{CEC}]}{\Delta t}$ and $\Delta E\left(\frac{\Delta[CEC]}{\Delta t}\right) \propto dE\left(\frac{d[CEC]}{dt}\right)$. We thus assume that induction due to concentration differences d[CEC] within dt (hours) is negligible as compared to Δt (months): [CEC] represents in situ concentrations that fed the WWTP in over longer periods of time (e.g., for months). Future work may distinguish between long-term background and real-time concentrations to refine analyses.

S5. Benchmarking activation energies

We can benchmark CEC activation energies on BOD activation energies. Taking Arrhenius, and second order kinetics for CECs:

Eq. S19 $$k_{CEC} = A_{CEC} \cdot e^{-\frac{\Delta G^{\ddagger}_{CEC}}{RT}}$$

Eq. S20 $$k = [E_{CEC}] \cdot k_{CEC}$$

And for BOD:

Eq. S21 $$k_{BOD} = A_{BOD} \cdot e^{-\frac{\Delta G^{\ddagger}_{BOD}}{RT}}$$

Eq. S22 $$k_{bio,BOD} = [E_{BOD}] \cdot k_{BOD}$$

We get by substitution and rearrangement:

Eq. S23 $$\frac{k}{k_{bio,BOD}} \cdot \frac{[E]_{BOD}}{[E]_{CEC}} = \frac{A_{CEC}}{A_{BOD}} \cdot e^{\frac{-\Delta G^{\ddagger}_{CEC} + \Delta G^{\ddagger}_{BOD}}{RT}}$$

Which is equivalent to:

Eq. S24 $$\Delta G^{\ddagger}_{CEC} = -RT \cdot ln\left(\frac{k}{k_{bio,BOD}} \cdot \frac{[E]_{BOD}}{[E]_{CEC}} \cdot \frac{A_{BOD}}{A_{CEC}}\right) + \Delta G^{\ddagger}_{BOD}$$

Which can be used as a benchmark to acquire activation energies for CECs $\Delta G^{\ddagger}_{CEC}$, based on comparison of experimental pseudo first order rate constants and the relative levels of acclimation $\frac{[E]_{BOD}}{[E]_{CEC}}$ (anything over 1, implying lower acclimation than for BOD), while knowing $\Delta G^{\ddagger}_{BOD}$ (e.g., 15-25 kJ/mol). Frequency factors $\frac{A_{BOD}}{A_{CEC}}$, describing interactions with E, depend on size and geometry [54]. As lipids, carbohydrates, etc. (i.e., BOD) are similar in size to some CECs, $\frac{A_{BOD}}{A_{CEC}} \approx 1$. Natural substances (nutrients), have higher uptake (induction of transporters, etc., [E]) [52, 60]. For realistic situations and experiments we see that $ln\left(\frac{k}{k_{bio,BOD}} \cdot \frac{[E]_{BOD}}{[E]_{CEC}} \cdot \frac{A_{BOD}}{A_{CEC}}\right)$ attains a negative value, so that $\Delta G^{\ddagger}_{CEC} > \Delta G^{\ddagger}_{BOD}$. *E.g.,* $\Delta G^{\ddagger}_{CEC}$, = -2.3·ln(1·10^{-8})+20 ≈ 65.4 kJ/mol, equal to the EFSA benchmark we used (S3).

S6. Supplemental modelling results

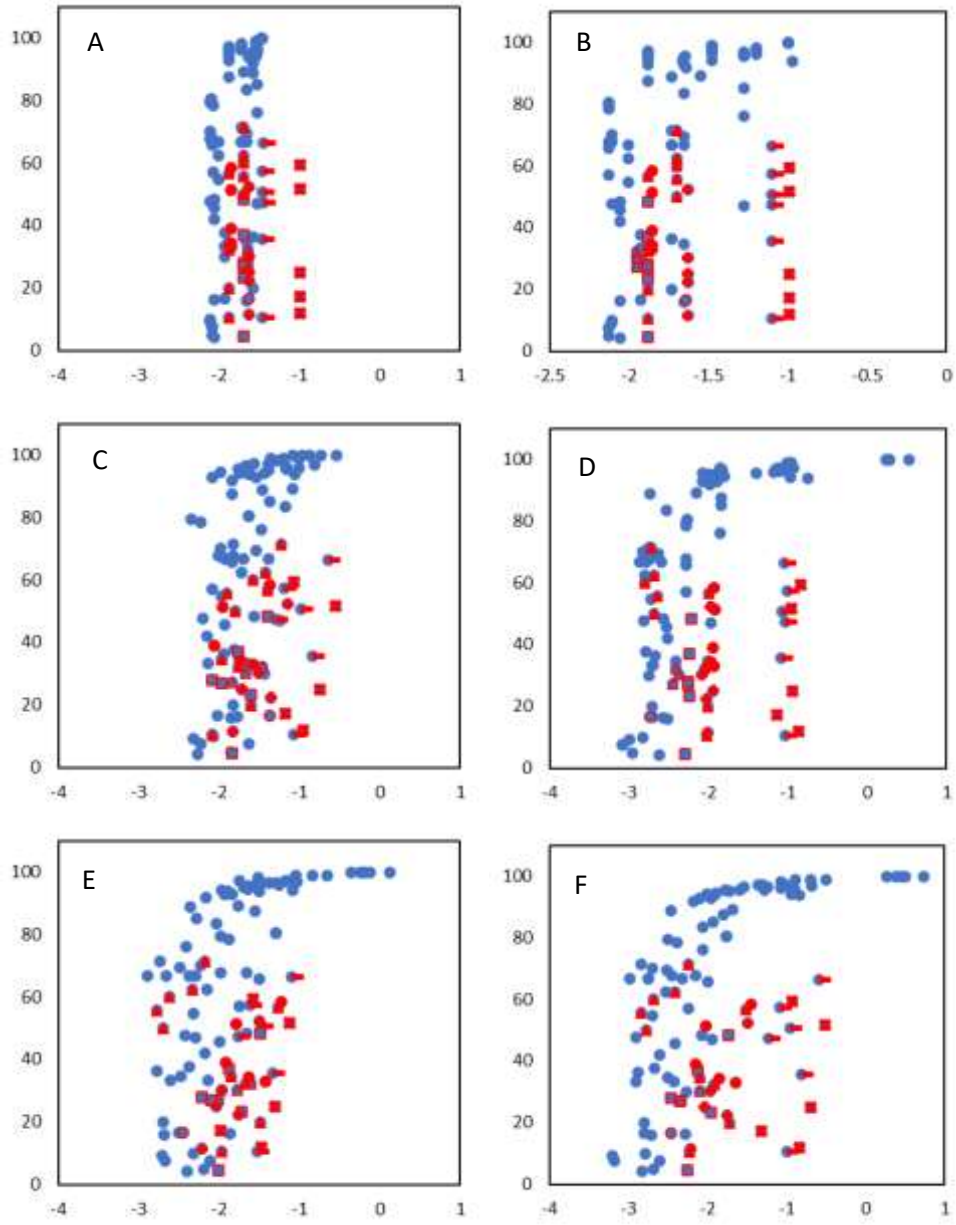

Figure S9. Observed removal (y-axis, in %) versus predicted pseudo first order biodegradation rate constant (h^{-1}, log-transformed). Data selection.

A: without acclimation (y[CEC]), influent temperature, $\Delta G^{\ddagger}_{CEC}$. / with A_{CEC}

B: without acclimation (y[CEC]), influent temperature. / with A_{CEC} and $\Delta G^{\ddagger}_{CEC}$

C: without acclimation (y[CEC]). / with A_{CEC}, $\Delta G^{\ddagger}_{CEC}$ and influent temperature

D: without influent temperature. / with A_{CEC}, $\Delta G^{\ddagger}_{CEC}$ and acclimation

E: without $\Delta G^{\ddagger}_{CEC}$ and A_{CEC}. / with influent temperature and acclimation

F: including all parametrizations. / with A_{CEC}, $\Delta G^{\ddagger}_{CEC}$, influent temperature and acclimation

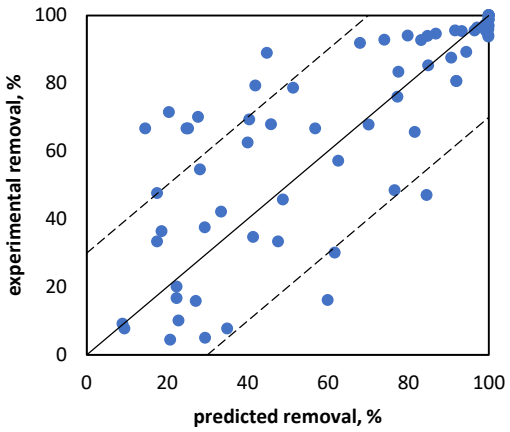

269

270 Figure S9B. Observed removal (y-axis, in %) versus predicted removal (y-axis, in %) based on log-logistic fit. Including all parametrizations. /
271 with A_{CEC}, $\Delta G^{\ddagger}_{CEC}$, influent temperature and acclimation.

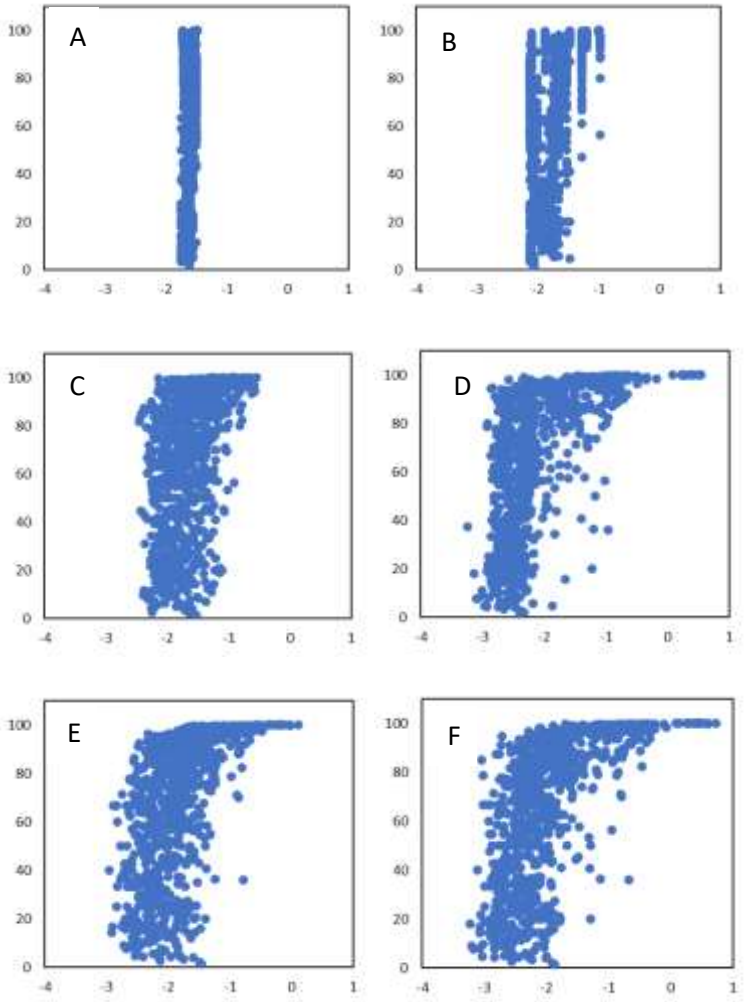

Fig. S10. Observed removal (y-axis, in %) versus predicted pseudo first order biodegradation rate constant (h^{-1}, log-transformed). All data.

A: without acclimation (y[CEC]), temperature, $\Delta G^{\ddagger}_{CEC}$.

B: without acclimation (y[CEC]), temperature.

C: without acclimation (y[CEC]).

D: without temperature.

E: without $\Delta G^{\ddagger}_{CEC}$ and A_{CEC}.

F: including all parametrizations.

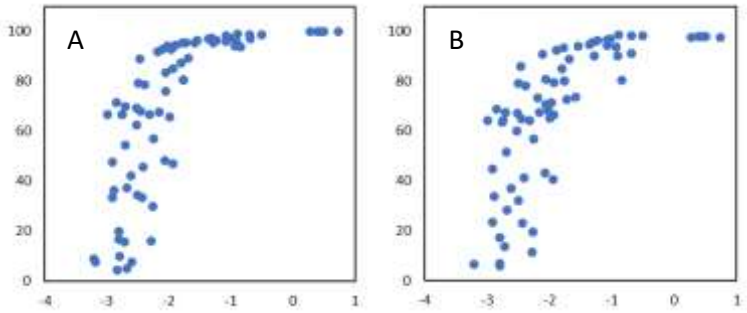

287

288 Fig. S11 Predicted log k (x-values) versus observed WWTP CEC removals (y) without (A: R^2=0.65) and with (B: R^2=0.60)
289 subtracting (T-dependent, pH-dependent) removal due to sorption in primary settling tank from WWTP total removals.

290

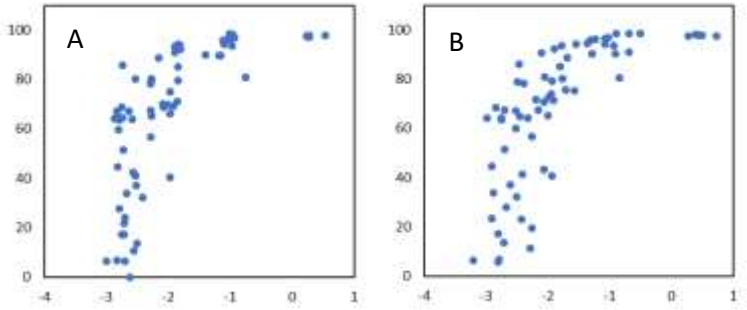

291

292 Fig. S12 Predicted log k (x-values) versus observed WWTP CEC removals (y) with subtracting percentages of removal via
293 sorption in primary settling tank of the WWTP. Sorption percentages calculated without temperature-dependence (A:
294 R^2=0.62) and pH-dependence (B: R^2=0.61).

295

S7. Back-transformation

To dose the effective concentration of (i.e., deactivate) drugs, the human body (liver) produces hydrophilic (e.g., glucuronide and sulfate) conjugates that more rapidly exit the body [61]. Whereas >99% of gut bacteria are anaerobes [62], conditions shift in the WWTP as these promote selection and promotion of oxygeneous bacteria and pathways that may utilize e.g. glucuronidates [63]. As a result, we investigated potential back-transformation reactions therein [64], by calculating removals in WWTP aeration (secondary) tanks via:

$$removal = \frac{[CEC]_{inf,a} - (1-f)[CEC]_{eff,a}}{[CEC]_{inf,a}}$$

Here, $f \cdot [CEC]_{eff}$ are concentrations of parent (p) CECs produced (back-transformed) in the WWTP's aeration (a) tanks. With $f_{p \to m,human}$ as the fraction of parent CEC transformed into metabolite (m) in human and $f_{m \to p,wwtp}$ the fraction of metabolite back-transformed into parent in the WWTP. With:

$$f = f_{p \to m,human} \cdot f_{m \to p,wwtp} = \frac{1}{1 + \left(\frac{[CEC]_{human}}{[CEC]_{human,\mu}}\right)^{-\beta_{human}}} \cdot \frac{1}{1 + \left(\frac{[CEC_m]_{influent}}{[CEC_m]_{influent,\mu}}\right)^{-\beta_{influent}}}$$

with a fitted scaling factor β = 3 (cumulative log-normal fits in previous sections), as WWTP bacteria are primarily of human origin [65] (bacteria make up <60% of fecal dry mass [66]) we take $\beta_{human} = \beta_{influent}$. $[CEC]_{human,\mu}$ is a generic population-average therapeutically effective half-saturation constant in plasma which, considering the common origin of (gut) bacteria, we take as $[CEC]_{human,\mu} = [CEC]_{influent,\mu}$ = 0.1 nM, representing marginal selectivity [67]. Due to a lack of experimental data, we simplified, taking the value for all CECs, while obviously differences exist [68].

$[CEC]_{human}$ is a population-wide average (therapeutically) relevant concentration of the CEC in human plasma: the more people use it (at a prescribed constant dosing), the higher the $[CEC]_{influent}$, by which we assume CEC_{human_μ} and CEC_{human} are optimized towards each other in each individual human (the more drug in plasma, induces higher μ) [68], Fig. 12-2B. We assume a maximum of 50% biotransformations:

$$[CEC_m]_{influent} = \frac{[CEC]_{influent}}{1 + \left(\frac{[CEC]_{human}}{[CEC]_{human,\mu}}\right)^{-\beta_{human}}}$$

$$[CEC]_{human} = \frac{d \cdot [CEC]_{influent}}{1 + \left(\frac{d \cdot [CEC]_{influent}}{[CEC]_{human,\mu}}\right)^{-\beta_{human}}}$$

d is a dilution factor (default = 1). Ranges calculated for $f_{p->m,human}$, affected by dosing [68], match those for experiments [69, 70]. The full constructed graph of Figure 11 (in the main document) is given below.

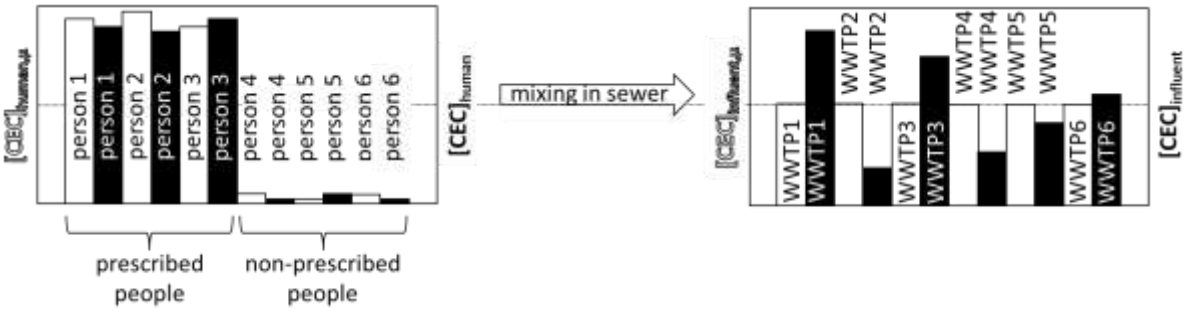

Fig. 12-2A. We assume a constant μ across WWTPs. The ratio between $cec_{human}/cec_{human,mu}$ and $cec_{influent}/cec_{inluent,mu}$ is constant.

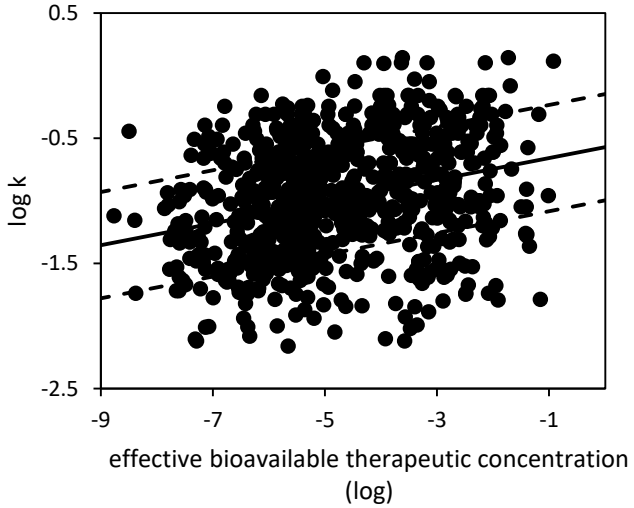

Fig. 12-2B. Relationship between clearance rate constant (hr^{-1}, log) and the effective bioavailable therapeutic concentration. Data from Schulz et al. [71]. The relationship is logk = 0.09 · log concentration – 0.57, with R^2 = 0.07. Half-life refers to cleansing through liver functioning and excretion through the kidneys and intestines. Dashed lines denote measurement variability in log k, 0.43. Additional intraspecies uncertainty factors of one or half an order of magnitude commonly apply [72, 73] .

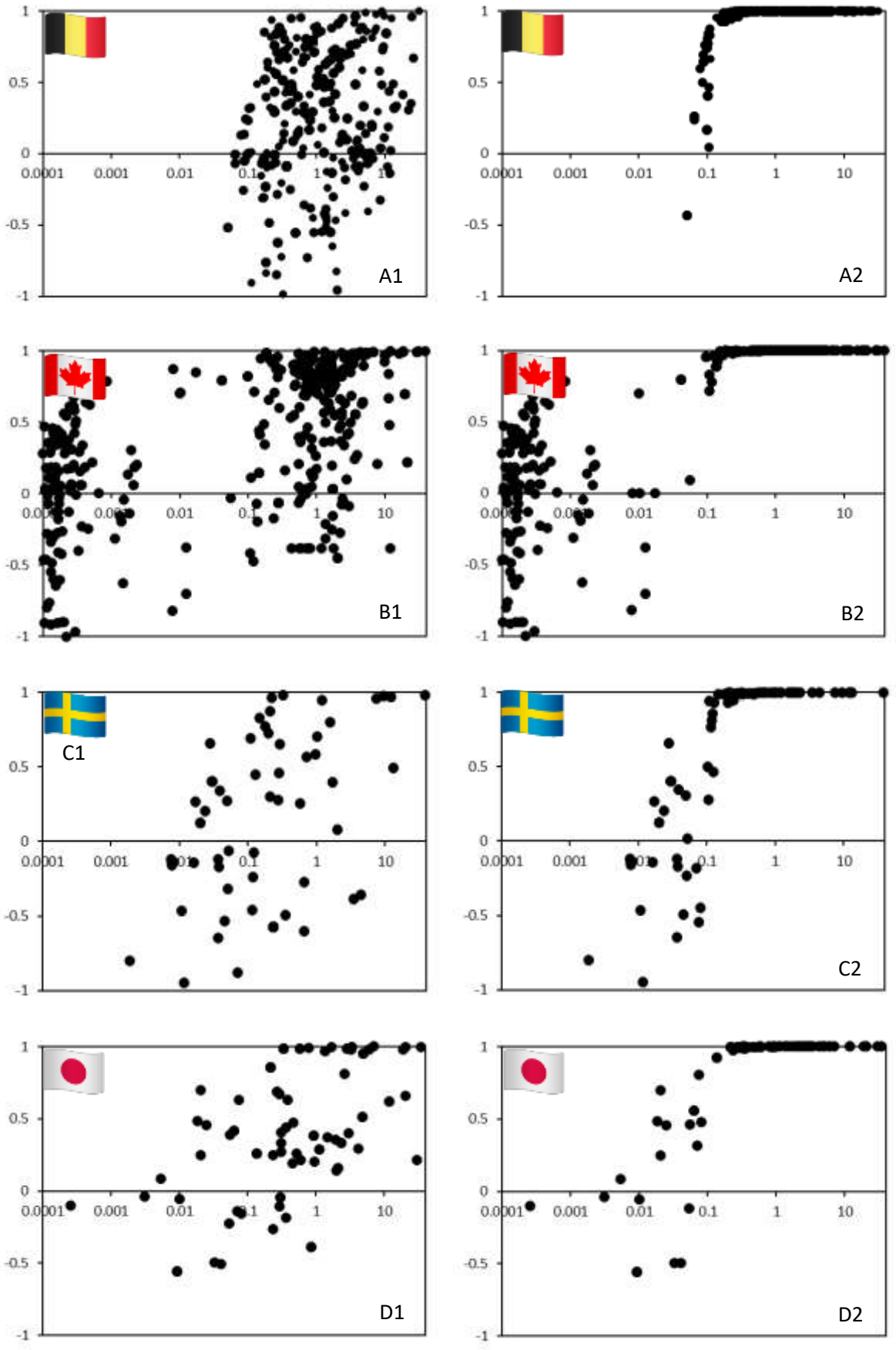

Fig. S13. CEC removal (fraction, y-axis) versus concentration (nM, x-axis). f=0 (S13-1), and calculated f (>0, S13-2). We deleted all Belgian CEC concentration values reported as lower than the detection limit, and those outlying the CEC log-average among all Belgian WWTPs by more than 2σ (>95%). 0.1 nM from [67] appears as a 'concentration limit'.

Outliers in Figure S13 include (super)hydrophobic (e.g., halogenated flame-retardants; logK_{OW}>4). These hardly enter aeration tanks (low concentrations, Fig. S13) because of removal via sedimentation/sorption beforehand. Outliers then attribute to variable sorption rendering concentrations in aeration uncertain (see also K_{OC} of clarithromycin and roxithromycin [74]). The longer and more chemicals reside in the environment, the more they will (have) induce(d) corresponding metabolic machinery with lower IC50 values: compare e.g., 'first generation' (~1950-1960s) herbicides to 'next generation' pharmaceuticals. Fluctuations in (day-to-day) concentrations of CECs, e.g., around holidays [75, 76], may give rise to concentrations that do not correspond (represent) the in-situ acclimation state.

REFERENCES

1. Donten, M.L., J. Vandevondele, and P. Hamm, *Speed limits for acid-base chemistry in aqueous solutions.* Chimia (Aarau), 2012. **66**(4): p. 182-6.
2. Lijklema, L., *Factors affecting pH change in alkaline wastewater treatment - II. Carbon dioxide production.* Water Research, 1971. **5**: p. 123-142.
3. Nolte, T.M., et al., *Nitrogen-chromium interactions driving Hyalella azteca mortality when exposed to Flanders' sediments.* in preparation, 2020.
4. C. B. Ong, et al., *Pilot study for sewage wastewater reclamation and reuse using RO membrane: comparison of different pre-treatment systems.* Desalination and Water Treatment, 2014. **54**(4-5): p. 1-8.
5. J. Sudthanom and S.F. AliZaidi, *To analyze the relationship between BOD, nitrogen and phosphorus contents at constant dissolved oxygen concentration in municipal wastewater treatment*, in *School of Sustainable Development of Society and Technology. Malardalen University Sweden*. 2011.
6. S. Karthikeyan, et al., *Characterization of iron impregnated polyacrylamide catalyst and its application to the treatment of municipal wastewater.* RSC Adv., 2013. **3**: p. 15044-15057.
7. Flegal, T.M. and E.D. Schroeder, *Temperature effects on BOD stoichiometry and oxygen uptake rate.* J Water Pollut Control Fed, 1976. **48**(12): p. 2700-7.
8. Hoshino, S. and H. Kubota, *Wastewater treatment with rotating biological contactor.* Wat. Purific. Liq. Waste Treatment, 1977. **18**(1): p. 29-35.
9. Gonzalez-Benitez, N., et al., *Drivers of Microbial Carbon Fluxes Variability in Two Oligotrophic Mediterranean Coastal Systems.* Sci Rep, 2019. **9**(1): p. 17669.
10. A.J., H., *Chapter 7: Organisms*, in *Syllabus for Environmental and Ecological Modelling. The power of size. Modelling (substances in) geo-hydrological, biological and social systems based on cross-disciplinary (scaling) principles*. 2016. p. 79.
11. H. Y. Hu, K. Fujie, and K. Urano, *Effect of Temperature on the Reaction Rate of Bacteria Inhabiting the Aerobic Microbial Film for Wastewater Treatment.* Journal of Fermentation and Bioengineering, 1994. **78**(1): p. 100-104.
12. J. Leithold, et al., *Quali-quantitative characterization of organic matter in urbanized drainage basins as a basis for the application of Water Resources Management Instruments.* RBRH, 2017. **22**(e55).
13. Lijklema, L., *Factors affecting pH change in alkaline waste water treatment - I.* Water Research, 1969. **3**: p. 913-930.
14. Evenblij, H., E. Schuman, and M. Kuiper, *Verwijderingsrendementen van medicijnresten op 18 rwzi's. WDOD database.* Water Matters, 2020. **28-31**.
15. Agency, E.U.S.E.P., *Greenhouse Gas Emissions Estimation Methodologies for Biogenic Emissions from Selected Source Categories: Solid Waste Disposal Wastewater Treatment Ethanol Fermentation*, M.P.G. RTI International to the Sector Policies and Programs Division, US EPA, EPA Contract No. EP-D-06-118., Editor. 2010. p. 596.
16. Cakir, F.Y. and M.K. Stenstrom, *Greenhouse gas production: a comparison between aerobic and anaerobic wastewater treatment technology.* Water Res, 2005. **39**(17): p. 4197-203.
17. Chai, C., et al., *Carbon Footprint Analyses of Mainstream Wastewater Treatment Technologies under Different Sludge Treatment Scenarios in China.* Water, 2015. **7**: p. 918-938.
18. Das, S., *Estimation of Greenhouse Gases Emissions from Biological Wastewater Treatment Plants at Windsor Wastewater Treatment Plants at Windsor*, in *Civil and Environmental Engineering*. 2011, University of Windsor.
19. R. H. R. Costa, et al. *Does Duckweed Ponds Used for Wastewater Treatment Emit or Sequester Greenhouse Gases (GHG)?* in *University of Leeds. 11th IWA Specialist Group Conference on Wastewater Pond Technology*. 2016.

20. Delft, T., *Aeration and gas stripping. Course subject(s) 03 – Aeration and gas stripping. Chapter 8 - Aeration and gas stripping. Drinking Water Treatment 1. TU Delft OpenCourseWare*.
21. Speece, R.E. and M.J. Humenick, *Carbon Dioxide Stripping from Oxygen Activated Sludge Systems.* Water Pollution Control Federation, 1973. **45**(3): p. 412-423.
22. Y. Cohen and H. Kirchmann, *Increasing the pH of Wastewater to High Levels with Different Gases—CO2 Stripping.* Water, Air, and Soil Pollution, 2004. **159**: p. 265–275.
23. Sander, R., *Compilation of Henry's law constants (version 4.0) for water as solvent.* Atmos. Chem. Phys., 2015. **15**(8): p. 4399–4981.
24. B. Mansouri, M. Ebrahimpour, and R. Baramaki, *Seasonal differences in treatmentefficiency of a set of stabilization ponds in a semi-arid region.* Toxicology and environmental chemistry, 2011. **93**(10): p. 1918-1924.
25. Tebes-Stevens, C.L. and W.J. Jones, *Estimation of microbial reductive transformation rates for chlorinated benzenes and phenols using a quantitative structure-activity relationship approach.* Environmental Toxicology and Chemistry, 2004. **23**(7): p. 1600-1609.
26. Nolte, T.M., et al., *Disentanglement of the chemical, physical, and biological processes aids the development of quantitative structure-biodegradation relationships for aerobic wastewater treatment.* Science of the Total Environment, 2020. **708**.
27. *Wet Weather Design and Operation in Water Resource Recovery Facilities. Chapter 12: Primary Treatment*. 2014, Water Environment Federation 601 Wythe Street Alexandria, VA 22314-1994 USA http://www.wef.org: WEF Special Publication.
28. Canada, E., *Atlantic Canada Wastewater Guidelines Manual for Collection, Treatment, and Disposal*. 2006.
29. Maktabifard, M., E. Zaborowska, and J. Makinia, *Achieving energy neutrality in wastewater treatment plants through energy savings and enhancing renewable energy production.* Reviews in Environmental Science and Bio/Technology, 2018. **17**: p. 655–689.
30. T. Bersinger, et al., *Assessment of erosion and sedimentation dynamic in a combined sewer network using online turbidity monitoring.* Water Science & Technology, 2015. **72.8**: p. 1375.
31. Georgaki, I., A. Dudeney, and A. Monhemius, *Characterisation of iron-rich sludge: correlations between reactivity, density and structure.* Minerals Engineering, 2004. **17**(2): p. 305-316.
32. S. Lombardo and W. Thielemans, *Thermodynamics of adsorption on nanocellulose surfaces.* Cellulose, 2019. **26**(1).
33. Dragan, A.I., C.M. Read, and C. Crane-Robinson, *Enthalpy-entropy compensation: the role of solvation.* Eur Biophys J, 2017. **46**(4): p. 301-308.
34. Molinspiration. *Molinspiration Cheminformatics*. Available from: http://www.molinspiration.com/.
35. A. W. Marczewski, et al., *Adsorption equilibrium and kinetics of selected phenoxyacid pesticides on activated carbon: effect of temperature.* Adsorption, 2016. **22**: p. 777-790.
36. J. A. Villamil, et al., *Potential Use of Waste Activated Sludge Hydrothermally Treated as a Renewable Fuel or Activated Carbon Precursor* Molecules, 2020. **25**(15): p. 3534.
37. Lopez-Capel, E., et al., *Chapter 3: Biochar properties*, in *Biochar in European Soild and Agriculture. Science and Practice*. 2016, Earthscan from Routledge.
38. Struijs, J., *SimpleTreat 4.0: a model to predict the fate and emission of chemicals in wastewater treatment plants. Background report describing the equations. RIVM Report 601353005/201*. 2014, RIVM.
39. *National Reserach Council. Use of Reclaimed Water and Sludge in Food Crop Production. Chapter 4*. 1996.
40. Golovko, O., et al., *Occurrence and removal of chemicals of emerging concern in wastewater treatment plants and their impact on receiving water systems.* Science of The Total Environment, 2021. **754**(142122).

41. Milo, R. and R. Phillips, *Cell Biology by the numbers*. 2016, New York, US: Garland Science.
42. Kilislioglu, A. and B. Bilgin, *Thermodynamic and kinetic investigations of uranium adsorption on amberlite IR-118H resin.* Appl Radiat Isot, 2003. **58**(2): p. 155-60.
43. W. Mrozik, et al., *Determination of the adsorption mechanism of imidazolium-type ionic liquids onto kaolinite: Implications for their fate and transport in the soil environment.* Environmental Chemistry, 2008. **5**(4): p. 299-306.
44. Ahmed, R., et al., *Sorption Behaviour of Lead(II) Ions from Aqueous Solution onto Haro River Sand.* Adsorption Science & Technology, 2006. **24**(6).
45. TGD, *Technical Guidance Document on Risk Assessment part 3. Commission Regulation (EC) No 1488/94 on Risk Assessment for existing substances*.
46. Hendriks A.J., T.T.P., Huijbregts M.A.J., *Critical body residues linked to octanol-water partitioning, organism composition, and LC50 QSARs: Meta-analysis and model.* Environ. Sci. Technol., 2005. **39**(9): p. 1803-1808.
47. Franco, A. and S. Trapp, *Estimation of the soil-water partition coefficient normalized to organic carbon for ionizable organic chemicals.* Environmental Toxicology and Chemistry, 2008. **27**(10): p. 1995-2004.
48. OECD, *OECD Guideline for Testing of Chemicals: Ready Biodegradability, OECD test 301*. 1992.
49. OECD, *OECD GUIDELINE FOR THE TESTING OF CHEMICALS. Aerobic Mineralisation in Surface Water – Simulation Biodegradation Test 309*. 2004.
50. EFSA, *Opinion on a Request from EFSA Related to the Default Q 10 Value Used to Describe the Temperature Effect on Transformation Rates of Pesticides in Soil. EFSA J. 636 2007, 622, 1–32.*
51. Wang, J., et al., *A generic Physiologically Based Kinetic Model for generic fish for assessment and prioritization of environmental risks of pharmaceuticals.* Environ. Sci. Technol. under review, 2021.
52. O'Connor, I.A., et al., *Including carrier-mediated transport in oral uptake prediction of nutrients and pharmaceuticals in humans.* Environ Toxicol Pharmacol, 2014. **38**(3): p. 938-47.
53. I. A. O'Connor, et al., *Modelling the oral uptake of chemicals - the role of plastic, passive diffusion and transport proteins. Chapter 6: Including Carrier-Mediated Transpoty in Oral Uptake Prediction of Nutrients and Pharmaceuticals in Humans, and Appendix Figure A6.4.1.* 2014, Radboud University: Nijmegen.
54. Nolte, T.M., et al., *Transition-state rate theory sheds light on 'black-box' biodegradation algorithms.* Green Chemistry, 2020. **22**(11): p. 3558-3571.
55. Nolte, T.M., et al., *Quantitative structure-activity relationships for primary aerobic biodegradation of organic chemicals in pristine surface waters: starting points for predicting biodegradation under acclimatization.* Environmental Science-Processes & Impacts, 2018. **20**(1): p. 157-170.
56. Olsen, K.N., et al., *Noninvasive measurement of bacterial intracellular pH on a single-cell level with green fluorescent protein and fluorescence ratio imaging microscopy.* Appl Environ Microbiol, 2002. **68**(8): p. 4145-7.
57. Nolte, T.M., et al., *Stoichiometric ratios for biotics and xenobiotics capture effective metabolic coupling and acclimation to re(de)fine biodegradation* Water Research, accepted, 2022.
58. Soubane, D., et al., *Hidden Information, Energy Dispersion and Disorder: Does Entropy Really Measure Disorder?* World Journal of Condensed Matter Physics, 2018. **8**(4).
59. Harb, M. and P.Y. Hong, *Molecular-based detection of potentially pathogenic bacteria in membrane bioreactor (MBR) systems treating municipal wastewater: a case study.* Environ Sci Pollut Res Int, 2017. **24**(6): p. 5370-5380.

60. O'Connor, I.A., et al., *Predicting the oral uptake efficiency of chemicals in mammals: Combining thehydrophilic and lipophilic range.* Toxicology and Applied Pharmacolog, 2013. **266**: p. 150–156.
61. Talevi, A. and B. C.L., *4.2.2 Synthetic (Phase II) Reactions*, in *ADME Processes in Pharmaceutical Sciences: Dosage, Design, and Pharmacotherapy Success*. 2018, Springer.
62. Sherwood, L., J. Willey, and C. Woolverton, *Prescott's Microbiology (9th ed.)*. 2013, New York: McGraw Hill.
63. Pellock, S.J. and M.R. Redinbo, *Glucuronides in the gut: Sugar-driven symbioses between microbe and host.* J Biol Chem, 2017. **292**(21): p. 8569-8576.
64. Zheng, W., et al., *Fate of estrogen conjugate 17alpha-estradiol-3-sulfate in dairy wastewater: comparison of aerobic and anaerobic degradation and metabolite formation.* J Hazard Mater, 2013. **258-259**: p. 109-15.
65. Wery, N., et al., *Human-specific fecal bacteria in wastewater treatment plant effluents.* Water Res, 2010. **44**(6): p. 1873-83.
66. Stephen, A.M. and J.H. Cummings, *The Microbial Contribution to Human Faecal Mass.* Journal of Medical Microbiology, 1980. **13**(1): p. 45–56.
67. Vlot, A.H.C., et al., *Target and Tissue Selectivity Prediction by Integrated Mechanistic Pharmacokinetic-Target Binding and Quantitative Structure Activity Modeling.* AAPS J, 2017. **20**(1): p. 11.
68. Loscher, W. and D. Schmidt, *Experimental and Clinical Evidence for Loss of Effect (Tolerance)during Prolonged Treatment with Antiepileptic Drugs.* Epilepsia, 2006. **47**(8): p. 1253–1284.
69. Wishart, D.S., et al., *DrugBank: a knowledgebase for drugs, drug actions and drug targets.* Nucleic Acids Research, 2008. **36**: p. D901-D906.
70. Callegari, E., M.V.S. Varma, and R.S. Obach, *Prediction of Metabolite-to-Parent Drug Exposure: Derivation and Application of a Mechanistic Static Model.* Clin Transl Sci, 2020. **13**(3): p. 520-528.
71. Schulz, M., et al., *Revisited: Therapeutic and toxic blood concentrations of more than 1,100 drugs and other xenobiotics.* Critical Care, 2020. **24**(1): p. 195.
72. EPA, *Recommended Use of Body Weight3/4 as the Default Method in Derivation of the Oral Reference Dose. Office of the Science Advisor Risk Assessment Forum U.S. Environmental Protection Agency Washington, DC 20460. EPA/100/R11/0001.* 2013.
73. EPA, *Consideration of the FQPA safety factor and other uncertainty factors in cumulative rusk assessment of chemicals sharing a common mechanism of toxicity. Office of Pesticide Programs. U.S. Environmental Protection Agency. Washington D.C. 20460.* 2002.
74. Carballa, M., et al., *Determination of the solid-water distribution coefficient (Kd) for pharmaceuticals, estrogens and musk fragrances in digested sludge.* Water Res, 2008. **42**(1-2): p. 287-95.
75. Giordano, C., et al., *Summer holidays as break-point in shaping a tannery sludge microbial community around a stable core microbiota.* Sci Rep, 2016. **6**: p. 30376.
76. EPA, *Occurrence of Contaminants of Emerging Concern in Wastewater From Nine Publicly Owned Treatment Works*. 2009, United States Environmental Protection Agency: Washington, DC.